

TRNSYS Type 832 v5.10 „Dynamic Collector Model by Bengt Perers“ Updated Input-Output Reference

Michel Haller, 5 August 2014

based on previous work of

Bengt Perers, Chris Bales, Janne Paavilainen, Antoine Dalibard, Stefan Fischer,
Erik Bertram

Contents

| | | |
|----|--|----|
| 1 | Disclaimer | 2 |
| 2 | Introduction | 2 |
| 3 | Summary..... | 2 |
| 4 | Parameter-List..... | 2 |
| 5 | Input-List | 4 |
| 6 | Labels | 5 |
| 7 | Output-List | 5 |
| 8 | Basic Equations (Cmode = 1 or 3)..... | 5 |
| 9 | Calculation of transversal and longitudinal incidence angles | 9 |
| 10 | Multi-segment mode | 9 |
| 11 | Condensation gains | 11 |
| 12 | Stability criteria | 13 |
| 13 | License, source code, further development etc..... | 13 |
| 14 | Further development and updates | 13 |
| 15 | Literature | 14 |
| | Appendix 1: Installation | 15 |
| | Appendix 2: External files | 16 |
| | Appendix 3: Changelog | 17 |
| | Changes from V 4.00 to V 5.00..... | 17 |
| | Changes from V 3.10 to V 4.00..... | 17 |
| | Changes from V 3.08 to V 3.10..... | 17 |
| | Changes introduced with V 3.07 and V 3.08 | 18 |

1 Disclaimer

The SPF Institut für Solartechnik and HSR University of Applied Research refuse to accept any liability for direct or indirect damages of any kind that may result from the use of this simulation model and its implementation in computer code (drop in dll fro TRNSYS).

2 Introduction

The Type132 collector model has originally been programmed by Bengt Perers. Additional features have been added since by B. Hellström, Chris Bales and Stefan Fischer. The latest changes have been introduced by Michel Haller based on suggestions from Antoine Dalibard and Janne Paavilainen. Component model history:

Type132 – TRNSYS15 and older

Type232 – TRNSYS15

Type232 – TRNSYS16 legacy mode

Type832 – TRNSYS16 drop-in dll

Since the code has changed quite a bit during the years, and in particular new inputs and parameters have been introduced, a new documentation of the parameters, inputs and outputs is given here.

3 Summary

The basic equations used by the model are shown in Section 6 to 8. In the current proforma the 2-axis IAM (Incidence Angle Modifier) data can only be given as a table in a text file as this is the most convenient input for the average user. For other types of input one has to modify the TRNSYS deck file (.dck) directly with a text editor.

4 Parameter-List

| <i>Nr.</i> | <i>short</i> | <i>explanation</i> | <i>unit</i> | <i>range</i> |
|------------|--------------------------|--|----------------------|--------------|
| 1 | A | Collector field aperture area | m ² | [0;inf] |
| 2 | $\eta_0; F'(\tau\alpha)$ | Collector optical efficiency (at zero temp. difference and nominal conditions) for CMode = 1: Eta0 = Zero loss efficiency at normal incidence (-) for CMode = 2: tau-alpha = effective transmission absorptance product (-) for CMode = 3,4: = not used | [-] | [0;1] |
| 3 | K_d | IAM for diffuse radiation | [-] | [0;1] |
| 4 | a_1 | Linear heat loss coefficient | W/(m ² K) | [0;inf] |

| | | | | |
|----|------------|---|------------------------------------|------------|
| 5 | a_2 | Quadratic heat loss coefficient | W/(m ² K ²) | [0;inf] |
| 6 | $c_{w,hl}$ | Wind speed dependency of heat losses | J/(m ³ K) | [-inf;inf] |
| 7 | c_{IR} | Infrared radiation dependency of collector | ? | [-inf;inf] |
| 8 | C_{eff} | Specific effective thermal capacitance of the collector, including fluid Effective area specific heat capacity of the collector, for CMode = 1: including the fluid for CMode = 2: excluding the fluid | J/(m ² K) | [1;100000] |
| 9 | $c_{w,F}$ | Wind speed dependency of the zero heat loss efficiency | s/m | [0;inf] |
| 10 | cp | Specific heat capacity of the collector fluid | kJ/(kgK) | [0;inf] |
| 11 | β | Collector slope (tilt angle) | [°] | [-360;360] |
| 12 | CMode | Collector mode for CMode = 1: CEN 1-node model (absorber, collector and fluid = 1 thermal node) for CMode = 2: 2-node model (absorber, collector and fluid are two separate thermal nodes) for CMode = 3: CEN 1-node model with conversion area for CMode = 4: 2-node model with conversion area | [-] | [1;4] |
| 13 | wf | Wind speed factor if wind data is not measured in collector plane | [-] | |
| 14 | rf | Sky radiation factor ($rf = [1 + \cos(\beta)]/2$) for a standard climate file without horizon) | [-] | |
| 15 | OMode | Optical mode for OMode = 1: b0 equation for OMode = 2: b0 equation according to MFC for OMode = 3: Symmetrical Kb(theta) for OMode = 4: Asymmetric 2-axis Kb(theta) in external text file for OMode = 5: Asymmetric 2-axis Kb(theta) as parameters (See source code for details) for OMode = 6-10: see source code for details | [-] | [1;9] |
| 16 | Cfl | for CMode = 2 or 4: Effective heat capacity of the fluid content (J/m ² K) for CMode = 1 or 3: unused | J/(m ² K) | [0;inf] |
| 17 | UAbsfl | for CMode 2 or 4: UAabsfl, Heat transfer rate between absorber and fluid for CMode 1 or 3: unused | W/(m ² K) | [0;inf] |
| 18 | b0 | Angle dependence of the transmittance absorptance product (tau-alpha) for OMode = 1-3: b0, IAM as b0 (first order) and b1 (second order) function of (1/cos(theta/180)-1) for OMode = 4: unused for Omode > 4: check FORTRAN code | [-] | [-inf;inf] |

| | | | | |
|----|------------|---|----------------------|-------------|
| 19 | b1 | Angle dependence of the transmittance absorptance product (τ - α) for Omode = 3: b1, IAM as b0 (first order) and b1 (second order) function of $(1/\cos(\theta/180)-1)$ | [-] | [-inf;inf] |
| 20 | N_{seg} | Number of collector segments in flow direction for heat capacitance calculation (for simulation with small timesteps and/or high collector heat capacitance) | [-] | [1;100] |
| 21 | MoSeg | Mode for segmented heat loss calculation. MoSeg = 0: heat losses based on first segment inlet and last segment outlet (same heat loss for each segment). MoSeg = 1: heat losses based on each segments inlet and outlet temperature (different heat losses for different segments). | [-] | [0;1] |
| 22 | γ | collector azimuth angle: (negative is east, positive is west) used for calculation of θ_L and θ_T ; specify as 999 if θ_L and θ_T are inputs | degree | [-inf;+inf] |
| 23 | -- | nothing / free | | |
| 24 | MoCond | mode for condensation gain calculation: 0 = no cond. gains, 1 = method of Perers, 2 = method of Bertram | percent | [0;+1] |
| 25 | c_{cond} | additional coefficient for condensation gains – method of Perers, idally = 0.916 | m ³ K/kJ | |
| 26 | u_{int} | u-value of the absorber or material between fluid and surface of the absorber to ambient boundary for condensation gain calculation according to Bertram | W/(m ² K) | [0;+inf] |
| 27 | MoFrost | mode for calculation of frost gains. 0 = no calculation of condensation or frost gains below Tamb = 0°C, 1 = calculation of frost gains. | - | [0;+1] |

5 Input-List

| Nr. | short | explanation | unit | range |
|-----|-------------------------|--|-----------------------|-------------|
| 1 | ϑ_{in} | inlet temperature | C | [-inf;+inf] |
| 2 | \dot{m} | inlet mass flow rate | kg/h | [0;+inf] |
| 3 | ϑ_{amb} | ambient temperature | C | [-inf;+inf] |
| 4 | I_t | global radiation on collector plane | kJ/(hm ²) | [0;+inf] |
| 5 | I_d | incidence diffuse radiation on collector plane | kJ/(hm ²) | [0;+inf] |
| 6 | θ | incidence angle of beam radiation | deg | [0;+inf] |
| 7 | $u_{w,0}$ | wind speed | m/s | [0;+inf] |
| 8 | $I_{IR,0}$ | long wavelength radiation downwards from sky | kJ/(hm ²) | [0;+inf] |
| 9 | θ_T ; θ_Z | if collector azimuth angle γ = 999: incidence angle in transversal direction; if γ < 999: solar zenith angle, for calculation of θ_T ; and | degrees | [0;+inf] |

| | | | | |
|----|----------------------|--|----------------------|----------|
| | | θ_L | | |
| 10 | $\theta_L; \gamma_S$ | if $\gamma = 999$: incidence angle in longitudinal direction $\gamma < 999$: solar azimuth angle for calculation of θ_T ; and θ_L | degrees | [0;+inf] |
| 11 | RH_{amb} | relative humidity of the ambient air | percent | [0;+100] |
| 12 | p_{amb} | pressure of the ambient air | bar | [0;+inf] |
| 13 | u_{conv} | convective heat transfer coefficient to absorber for condensation gains calculation. Set to -1 for internal calculation | W/(m ² K) | [0;+inf] |

6 Labels

Label 1

absolute path of IAM-table file in case of Omode = 4

7 Output-List

| Nr. | short | explanation | unit | range |
|------------|------------------------|---|------------------|--------------|
| 1 | \mathcal{G}_{out} | collector outlet temperature | C | [-inf;+inf] |
| 2 | \dot{m} | collector outlet mass flow rate | kg/h | [0;+inf] |
| 3 | \dot{Q}_{out} | thermal energy gain | kJ/h | [-inf;+inf] |
| 4 | \mathcal{G}_{abs} | mean absorber temperature (only in CMode 2 and 4) | C | [-inf;+inf] |
| 5 | \dot{q}_{rad} | radiative energy gain per m2 | W/m ² | [-inf;+inf] |
| 6 | K_b | incidence angle modifier for beam radiation | - | [-inf;+inf] |
| 7 | θ_T | incidence angle in transversal direction | degree | [-inf;+inf] |
| 8 | θ_L | incidence angle in longitudinal direction | degree | [-inf;+inf] |
| 9 | | specific heat gain of collector (not equal to heat output) | W/m ² | [-inf;+inf] |
| 10 | | specific condensation gain | W/m ² | [0;+inf] |
| 11 | Qmtherm | total heat change rate of thermal capacitance | kJ/h | [-inf;+inf] |
| 12 | | energy balance error (Qgain-Qmtherm-Qout) | W | [-inf;+inf] |
| 21-120 | $\mathcal{G}_{out}(x)$ | outlet temperature of segments x = 1-100 during this timestep | °C | [-inf;+inf] |

8 Basic Equations (Cmode = 1 or 3)

Although for in-depth knowledge about the theoretical background of this model we refer to the original literature of Perers (2002), and ISO 9806-3, the basic equations are summarized here again for the quick reader:

$$\begin{aligned}
 \dot{q}_{out} = & F'(\tau\alpha) \cdot K_b \cdot I_b + F'(\tau\alpha) \cdot K_d \cdot I_d - c_{w,F'} \cdot u_w \cdot (I_b + I_d) + c_{IR} \cdot (I_{IR} - \sigma \cdot T_{amb}^4) \\
 & - a_1 \cdot \Delta T_{amb} - a_2 \cdot |\Delta T_{amb}| \cdot \Delta T_{amb} - c_{w,hl} \cdot u_w \cdot (\Delta T_{amb}) + \dot{q}_{lat} \\
 & - C_{eff} \cdot d\mathcal{G}_m / dt
 \end{aligned} \tag{1}$$

with; $\Delta T_{amb} = \mathcal{G}_m - \mathcal{G}_{amb}$; $u_w = wf \cdot u_{w,0}$; and $I_{IR} = rf \cdot I_{IR,0} + (1 - rf) \cdot \sigma \cdot T_{amb}^4$

\dot{q}_{out} heat output of the collector per area, Wm^{-2}

\dot{q}_{lat} latent (condensation + sublimation) heat gains, Wm^{-2}

$F'(\tau\alpha)$ zero loss efficiency of the collector, sometimes referred to as η_0 , -

K_b incidence angle modifier for beam radiation, -

I_b Beam radiation incident on collector plane, Wm^{-2}

K_d incidence angle modifier for beam radiation, -

I_d Diffuse radiation incident on collector plane, Wm^{-2}

$c_{w,F'}$ Factor for a wind dependency correction of F' (and thus the zero loss coefficient $F'(\tau\alpha)$), used for unglazed collectors, sm^{-1}

u_w wind speed parallel to the collector plane, ms^{-1}

a_1 first order heat loss coefficient, $\text{WK}^{-1}\text{m}^{-2}$

a_2 second order heat loss coefficient, $\text{WK}^{-2}\text{m}^{-2}$

\mathcal{G}_m arithmetic mean of the collector temperature, $^{\circ}\text{C}$

\mathcal{G}_{amb} ambient temperature at location of collector field, $^{\circ}\text{C}$

T_{amb} absolute ambient temperature at location of collector field, K

$c_{w,hl}$ wind speed dependency of heat losses, $\text{Jm}^{-3}\text{K}^{-1}$

c_{IR} long wave irradiation dependency of heat losses (or gains), -

I_{IR} long wave irradiation on collector plane, Wm^{-2}

σ Stefan Boltzmann constant, $\text{Wm}^{-2}\text{K}^{-4}$

t time, s

C_{eff} effective thermal capacitance of the collector (including fluid), $\text{Jm}^{-2}\text{K}^{-1}$

In the case of steady state ($d\mathcal{G}_m/dt$), normal incidence ($K_b = K_d = 1$), no dependencies on wind speed ($c_{w,F'} = 0$, $c_{w,hl} = 0$) or infrared radiation ($c_{IR} = 0$), and collector temperatures above ambient temperatures ($\Delta T_{amb} > 0$), equation (1) can be reduced to the well known steady state efficiency approximation:

$$\dot{q}_{out} = \eta_0 \cdot (I_b + I_d) - a_1 \cdot (\mathcal{G}_m - \mathcal{G}_{amb}) - a_2 \cdot (\mathcal{G}_m - \mathcal{G}_{amb})^2 \tag{2}$$

with

$$\eta_0 = F'(\tau\alpha) \quad (3)$$

The first line of equation (1) can be seen as a term describing the radiative balance of the collector. With the approximations chosen for the long wave heat exchange in this model, it does not depend on the collector temperature, and can be calculated independently from the collector temperature as:

$$\dot{q}_{rad} = F'(\tau\alpha) \cdot K_b \cdot I_b + F'(\tau\alpha) \cdot K_d \cdot I_d - c_{w,F} \cdot u_w \cdot (I_b + I_d) + c_{IR} \cdot (I_{IR} - \sigma \cdot T_{amb}^4) \quad (4)$$

The determination of the actual heat gain and collector output is an iterative process. In a first step, the actual collector heat gain with the inclusion of the temperature dependent thermal losses of the collector are calculated:

$$\dot{q}_{gain} = \dot{q}_{rad} - a_1 \cdot (\vartheta_m - \vartheta_{amb}) - a_2 \cdot (\vartheta_m - \vartheta_{amb})^2 - c_{w,hl} \cdot u_w \cdot (\vartheta_m - \vartheta_{amb}) + \dot{q}_{cond} \quad (5)$$

In a second step, the outlet temperature of the collector ϑ_{out} of this time step is calculated from the collector gain \dot{q}_{gain} , the average temperature of the collector during the last timestep $\vartheta_{m,old}$, the collector parameters, and the flow parameters of this timestep:

$$\vartheta_{out} = \frac{\left(\frac{\dot{m} \cdot cp \cdot \vartheta_{in}}{A} - \frac{C_{eff} \cdot \vartheta_{in}}{2 \cdot \Delta t} + \dot{q}_{gain} + \frac{C_{eff} \cdot \vartheta_{m,old}}{\Delta t} \right)}{\frac{\dot{m} \cdot cp}{A} + \frac{C_{eff}}{2 \cdot \Delta t}} \quad (6)$$

Which is a result of the energy balance:

$$\vartheta_{out} = \vartheta_{in} + \frac{\dot{q}_{gain} - \left(\frac{\vartheta_{in} + \vartheta_{out}}{2} - \vartheta_{m,old} \right) \cdot \frac{C_{eff}}{\Delta t}}{\dot{m} \cdot cp / A} \quad (7)$$

Where the average heat transfer to the collectors thermal capacitance is subtracted from the heat gain in order to get the heat output. $\vartheta_m = (\vartheta_{in} + \vartheta_{out})/2$ is used for the average temperature of the collectors thermal capacitance.

In the case of no mass flow, the change of the collector temperature is:

$$\vartheta_{out} = \vartheta_m = \vartheta_{m,old} + \dot{q}_{gain} \cdot \frac{\Delta t}{C_{eff}} \quad (8)$$

The above equations can cause troubles in simulations with small timesteps and/or high thermal capacitance. In particular, unstable outlet temperatures just after the collector loop pump starts or stops can be observed and may cause problems for control and solver algorithms. Thus the possibility of splitting the collector's thermal mass in a number of serial segments was introduced. In order to make sure that the steady state efficiency would still be in agreement with the collector test norms, the same ΔT_{amb} is used for all segments in steady state operation. However, when the mass flow stops, the temperature differences between the fluid in different segments would persist if all segments would have the same heat losses, causing the outlet temperature of the last segment to rise higher than the expected stagnation

temperature. Therefore, in cases of no mass flow the temperature difference to the ambient and respective heat losses are calculated for each segment separately. This also has the effect that the temperature differences between the segments disappear with time after the pump stops. A flow chart of the FORTRAN code is given in Figure 1.

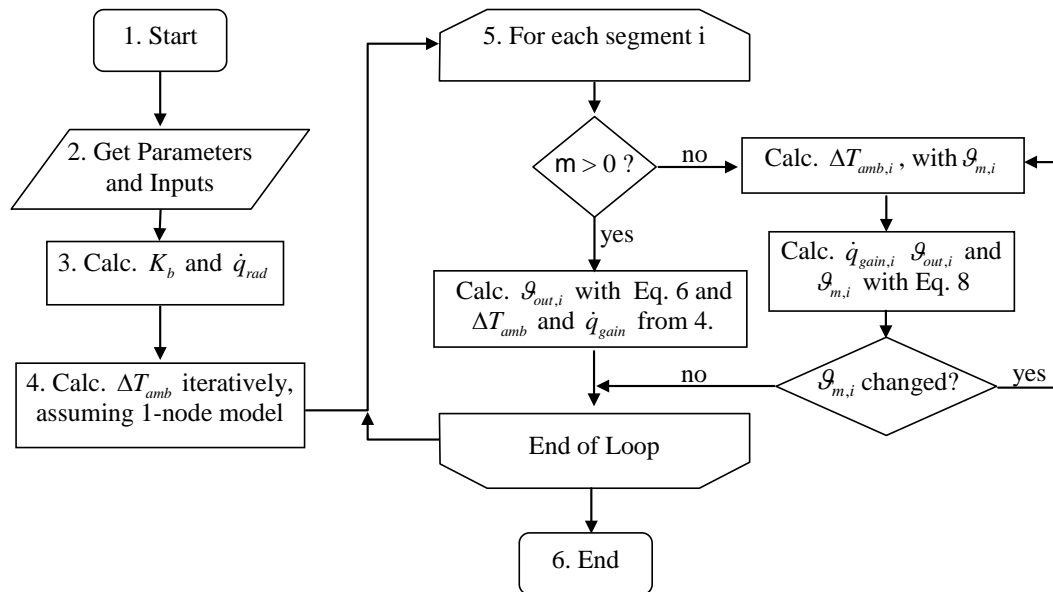


Figure 1: Flow Chart of the FORTRAN Program Code: Step 3 is only calculated once every timestep (no iteration).

9 Calculation of transversal and longitudinal incidence angles

For collectors whose incidence angle modifier in transversal direction differs from the one in longitudinal direction (e.g. vacuum tube collectors), the transversal and longitudinal components of the incidence angle have to be known separately. In this collector model these components may be given as inputs or they may be calculated internally based on data from the radiation processor of TRNSYS. The calculation of the transversal and longitudinal incidence angles is done based on equations from [Klein 1996], which had to be slightly adapted / corrected to produce the desired results in all cases, as reported in Heimrath & Haller (2007):

$$\theta_L = \left| ATAN \left(TAN(\theta_z) \cdot COS(\gamma - \gamma_s) \right) - \beta \right|$$

$$\theta_T = ATAN \left(\frac{SIN(\theta_z) \cdot SIN(|\gamma - \gamma_s|)}{COS(\theta)} \right)$$

| | |
|------------|---|
| θ_L | Angle of incidence on collector plane in longitudinal direction |
| θ_T | Angle of incidence on collector plane in transversal direction |
| θ_z | Solar zenith angle |
| γ | Collector azimuth angle |
| γ_s | Solar azimuth angle |
| θ | Angle of incidence on collector plane |
| β | Collector slope |

10 Multi-segment mode

The new approach of splitting up the collector into segments addresses some problems in the original model during transients. The problems were caused by the storage term (thermal capacitance and average temperature change between time steps) in combination with a linear temperature gradient resulting in that the model in some cases extrapolated unrealistic outlet temperatures from one time step to another, specifically with small time steps. This caused further problems with e.g. controllers and convergence. By dividing the collector into segments the temperature gradient is not linear for the whole collector. To avoid differences between the energy balance of this model in steady state and parameter identification based on equation (2), thermal loss calculation of a single segment with equation (5) uses the mean **collector** temperature for \mathcal{Q}_m under operating conditions. In the case of no fluid flow, the mean **segment** temperature is taken for \mathcal{Q}_m in thermal loss calculation to assure agreement of the models stagnation temperature with the theory. Compared to previous versions one can expect a difference in energy balance during transients,

but for steady state it should be the same as earlier. Thus, because of the difference in transient energy balance one can expect also differences for long simulations, depending on how much the system is working near steady state.

The difference in the results between one segment ($n=1$) and multiple segments ($n=2-10$) can be seen in Figure 2. General values of the simulation are listed in Table 1. The differences in heat gain between these simulations can be seen in Table 2.

Table 1: Values used for the TRNSYS test-simulation.

| parameter | value | units |
|--|---------|------------------------------------|
| collector area | 10 | m ² |
| zero loss efficiency η_0 (or $F'(\tau\alpha)$) | 0.8 | - |
| linear heat loss coefficient | 3.5 | Wm ⁻² K ⁻¹ |
| quadratic heat loss coefficient | 0.015 | Wm ⁻² K ⁻² |
| IAM for diffuse radiation K_d | 1.0 | - |
| specific mass flow | 0, 6, 8 | kg h ⁻¹ m ⁻² |
| collector effective capacitance | 7000 | Jm ⁻² K ⁻¹ |
| timestep | 0.05 | h |

The “unphysical” value of 1 is used for the IAM for diffuse radiation in order to simplify the validation of the changes introduced into the model. Extreme values are used for mass flow rate and capacitance for the same reason.

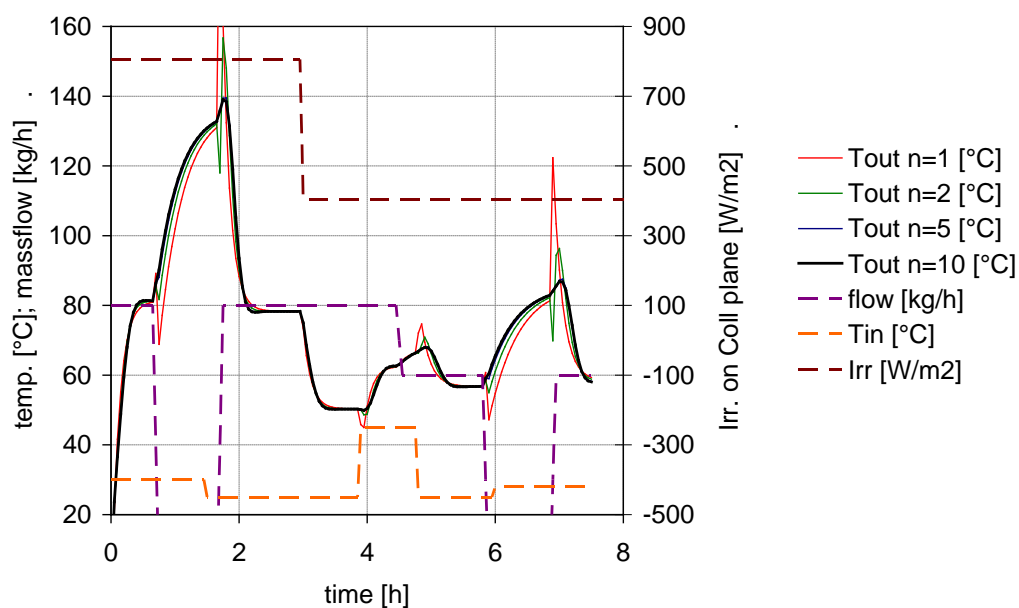


Figure 2: Simulation results for 1, 2, 5 and 10 nodes simulations.

Table 2: Differences in heat gains for 1, 2, 5, and 10 nodes.

| Simulation | Heat Gain (kWh) | Diff.to 1 node |
|----------------------------|-----------------|----------------|
| 1 node simulation (n=1) | 18.331 | 0% |
| 2 nodes simulation (n=2) | 18.258 | -0.4% |
| 5 nodes simulation (n=5) | 18.252 | -0.4% |
| 10 nodes simulation (n=10) | 18.251 | -0.4% |

11 Condensation gains

Two modes for the calculation of condensation gains have been implemented. For $MoCond = 0$, no condensation gains are calculated. $MoCond = 1$ is based on Perers (2010). In this mode, the condensation gains are calculated as:

$$\dot{q}_{lat} = c_{cond} \cdot \Delta h_{cond} \cdot u_{conv} \cdot \left[RH_{amb} / 100 \cdot \nu_{sat}(\vartheta_{amb}) - \nu_{sat}(\vartheta_m) \right] \quad (9)$$

with

c_{cond} a parameter to be identified for the particular absorber, ideally it corresponds to $Le^{-2/3} / (c_{p_l} \cdot \rho_l) = 0.916 [m^3 K / kJ]$, $m^3 K / kJ$

Δh_{cond} enthalpy of water condensation (depending on temperature 2400 – 2500 kJ/kg), for temperatures of the absorber fluid $< -1^\circ C$, the enthalpy of solidification (+333.5 kJ/kg) is added to this value, kJ/kg

u_{conv} convective heat transfer coefficient between ambient air and absorber surface for condensation gain calculation, may be an input or calculated internally, $W/m^2 K$

$wf \cdot u_{w,0}$ meteorological wind speed multiplied with wind speed factor to account for mitigation effects that lead to lower wind speed on the absorber surface, m/s

$\nu_{sat}(\vartheta)$ saturated water load of air at temperature ϑ , kg/m^3

The internal calculation of u_{conv} in the method of Perers is:

$$u_{conv} = 2.8 + 3.0 \cdot wf \cdot u_{w,0}$$

The second approach ($MoCond = 2$) is based on a method described by Bertram et al. (2010):

$$\dot{q}_{lat} = u_{conv} \cdot \Delta h_{cond} \cdot \frac{R_L}{R_D} \cdot \frac{Le^{-2/3}}{c_{p_l} \cdot p_{amb}} \cdot \left[RH_{amb} / 100 \cdot p_{sat}(\vartheta_{amb}) - p_{sat}(\vartheta_{surf}) \right] \quad (10)$$

$$\vartheta_{surf} = \vartheta_m + \dot{q}_{gain} / u_{int} \quad (11)$$

with

R_L / R_D ratio of gas constant of air and water vapour, -

p_{amb} ambient pressure, bar

$p_{sat}(\vartheta)$ saturation water vapour pressure at temperature ϑ , bar

u_{int} internal heat transfer coefficient between fluid and absorber surface – to be found for each collector, W/m^2K

The internal calculation of u_{conv} in this method is:

$$u_{conv} = \sqrt[3]{\left(0.123 \cdot (\vartheta_{surf} - \vartheta_{amb}) + 2.7\right)^3 + \left(2.83 \cdot wf \cdot u_{w,0} + 4.3\right)^3} \quad (12)$$

Difference of the two methods:

since $R_L \cdot p_{sat}(\vartheta) / (R_D \cdot p_{amb}) = v_{sat}(\vartheta) / \rho_l(\vartheta)$, the two methods are quite similar with the exception that the mean fluid temperature ϑ_m is used as a base for the calculation of the water vapor load on the collector surface in the first method (M1), whereas the absorber temperature ϑ_{surf} is estimated and used for the calculation of the water vapor pressure in the second method (M2). It is thus no surprise that for identical u_{conv} and an ideal $u_{int} = 10'000 W / (m^2 K)$, a factor c_{cond} can be found in a way that the results of the two models match ($RH_{amb} = 90\%$, Fig. Figure 3). However, for non-ideal $u_{int} = 10 W / (m^2 K)$, the onset of condensation is different for the two models because of the difference between the absorber temperature and the fluid temperature assumed in M2 (Figure 4).

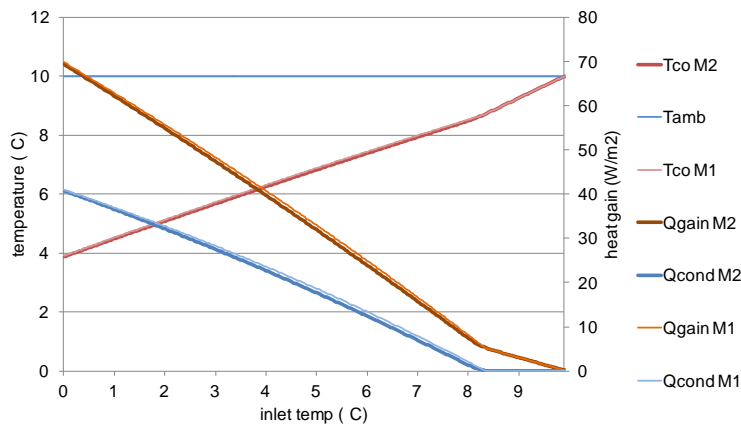


Figure 3: for large u_{int} , a u_{cond} can be found such that the two models match.

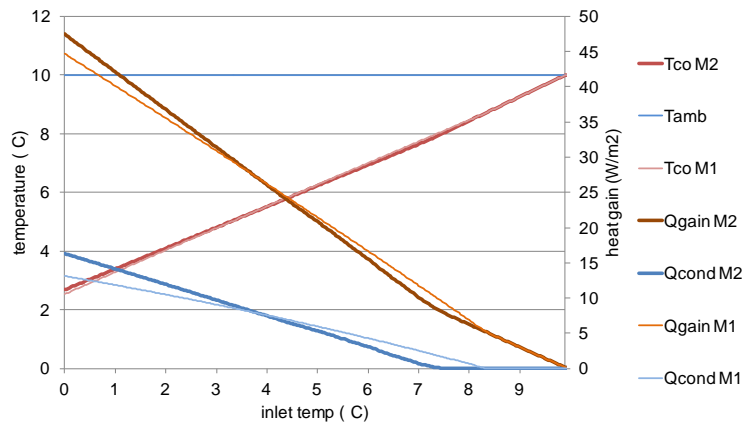


Figure 4: for a small $u_{int}=10 \text{ W/m}^2\text{K}$, no match is possible due to different onset of condensation.

12 Stability criteria

Depending on the parameters and inputs, the calculation of this type may become unstable. Therefore, the following stability criteria is checked whenever there is a mass flow:

$$\frac{\dot{m} \cdot c_p \cdot N_{seg} \cdot dt}{C_{eff} \cdot A} \geq 0.5 \quad (13)$$

A warning is printed to the log-file if the stability criteria is not met.

13 License, source code, further development etc.

The Type832 component is free of charge and no license is needed. The source code is open.

14 Further development and updates

The Type832 is not actively developed by any of the authors with exception for sporadic bugfixes and improvements. Bug reports can be sent to the authors and will be looked at when time and budget allows. The user can feel free to make own bugfixes and modifications to the source code. Also, to keep the maintenance and distribution centralized, user written modifications and bugfixes are kindly received by the authors to be included into future „official“ releases of the component to the general TRNSYS community.

15 Literature

Bertram, E., Glembin, J., Scheuren, J. & Rockendorf, G., 2010. Condensation Heat Gains on Unglazed Solar Collectors in Heat Pump Systems. In: Proc. of the EuroSun 2010 Conference, Graz, Austria.

Klein S.A., et al., TRNSYS 14.2 - A TRaNsient SYstem Simulation Program, Solar Energy Laboratory, University of Wisconsin-Madison, USA, 1996.

Fischer, S. & Müller-Steinhagen, H., 2007. Leistungsprüfung von Sonnenkollektoren - Kürzere Prüfzeiten durch die Verwendung eines 2-Knoten Modelles. In 17. Symposium Thermische Solarenergie. Kloster Banz, Bad Staffelstein, Germany, (German).

Heimrath, R. & Haller, M., 2007. Project Report A2 of Subtask A: The Reference Heating System, the Template Solar System - A Report of IEA SHC Task 32: Advanced storage concepts for solar and low energy buildings.

Perers, B., 1993. Dynamic method for solar collector array testing and evaluation with standard database and simulation programs. Solar Energy, 50(6), 517-526.

Perers, B. & Bales, C., 2002. A Solar Collector Model for TRNSYS Simulation and System Testing - A technical report of Subtask B of the IEA-SHC - Task 26.

Perers, B., 2010. An Improved Dynamic Solar Collector Model Including Condensation and Asymmetric Incidence Angle Modifiers. In: Proc. of the EuroSun 2010 Conference, Graz, Austria.

Appendix 1: Installation

The Type832 collector model is a TRNSYS16 drop-in dll component. For a complete set of files one should have:

The latest version of this manual

Type832vABC.dll – the drop-in dll file (release version)

Type832vABC.for – the FORTRAN source code

(where ABC is the version number)

Type832.tmf – the Simulation Studio proforma

Type832.bmp – the Simulation Studio proforma icon

IAM_Sample.iam – the example IAM input file

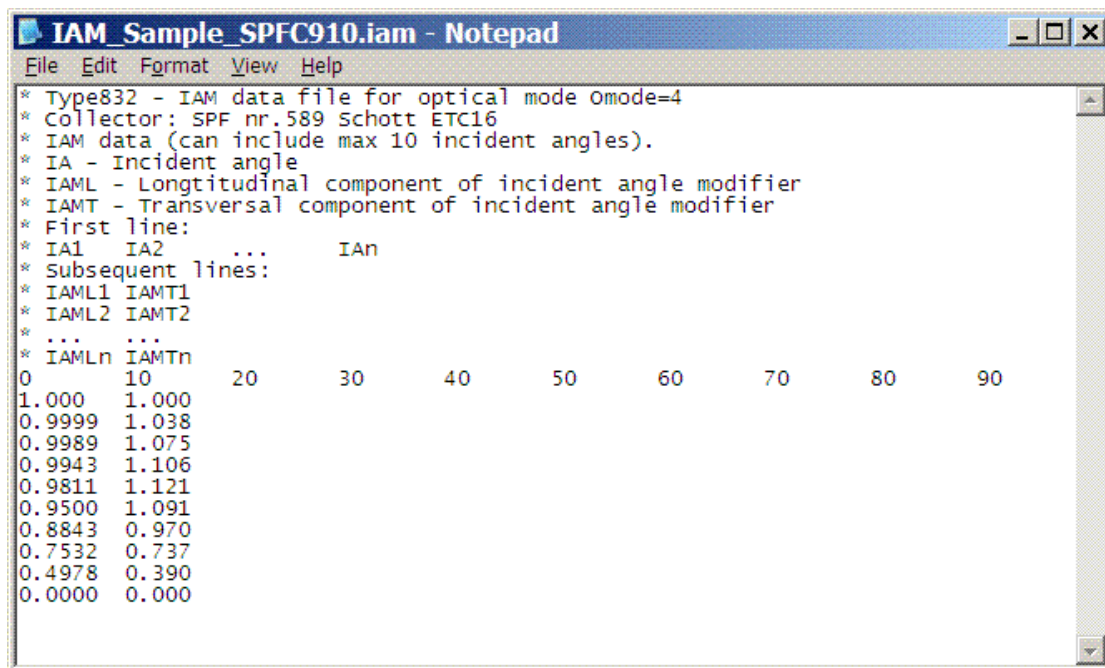
For installation:

1. Copy the .dll file to \TRNSYS16\UserLib\ReleaseDLLs\
2. Copy the .tmf and .bmp files to the \Proformas folder, e.g. C:\Trnsys16\Studio\Proformas\Nonstandard\
3. Restart simulation studio if it was running.
4. If you want to replace old components of the same Type in your project you will have to go through all instances by “Right-click→Replace” and check for possible lost connections.

The source code is for reference and further development and is not needed to run the component. An IAM input file is needed even if one does not simulate with optical mode Omode=4. This is because the simulation studio assigns a file handle automatically when it writes the deck file and thus TRNSYS will try to open the file even if it will not be used later. A dummy file can be used in this case. Note that the example IAM file is to show the format of the file and should not be treated as representative data for an average collector. For realistic IAM-data look for collector test results for the specific collector simulated.

Appendix 2: External files

The 2-axis IAM data can be given in a separate ASCII file. Multiple instances of the TYPE832 in the same project can use either the same input file or individual input files. The IAM can be given for a maximum number of 10 incidence angles. As interpolation is used the first incidence angle must be 0° and the last 90°. The file data content layout should be according to Figure 1. The number of comment lines is arbitrary.



```
* Type832 - IAM data file for optical mode Omode=4
* Collector: SPF nr.589 Schott ETC16
* IAM data (can include max 10 incident angles).
* IA - Incident angle
* IAML - Longitudinal component of incident angle modifier
* IAMT - Transversal component of incident angle modifier
* First line:
* IA1 IA2 ... IAn
* Subsequent lines:
* IAML1 IAMT1
* IAML2 IAMT2
* ...
* IAMLn IAMTn
0 10 20 30 40 50 60 70 80 90
1.000 1.000
0.9999 1.038
0.9989 1.075
0.9943 1.106
0.9811 1.121
0.9500 1.091
0.8843 0.970
0.7532 0.737
0.4978 0.390
0.0000 0.000
```

Figure 5: Text file format for 2-axis IAM data.

Note that an IAM input file is needed even if one does not simulate with optical mode Omode=4. This is because the simulation studio assigns a file handle automatically when it writes the deck file and thus TRNSYS will try to open the file even if it will not be used later. A dummy file can be used in this case.

Appendix 3: Changelog

Changes from v 5.01 to v 5.10

- Corrected a typo in eq. (1) and eq. (4): $+c_{IR}$ instead of $-c_{IR}$ in the documentation. The Fortran code is not affected as it always used $+c_{IR}$.
- Model correction / bugfix: added $+(1-r_f) \cdot \sigma \cdot T_{amb}^4$ to the calculation of I_{IR} that is used in eq. (1).
- Removed outdated reference to the use of parameters 40 -100 for IAM fitting purposes. This option has been removed from the code already before.

Documentation update on 14 Jan. 2014

- Corrected the description: the maximum number of nodes is 100 since version 3.10.

Changes from V 5.00 to V 5.01

- The "LABEL"-part of the TMF-File for the Studio has changed by Kai Schäfer (solites) since the "old" TMF-File did not work properly when Omode = 4 was chosen (reading iam-tables from input files).

Changes from V 4.00 to V 5.00

- A bug in 3.10 and 4.00 lead to increased collector gains due to wrong calculation of thermal capacitance temperature. This bug has been fixed.

Changes from V 3.10 to V 4.00

- A bug in 3.0X to 3.10 lead to inconsistent results if more than one unit of this type was used with different irradiation on the collector plane. This bug has been fixed. All previous multinode – version were not suitable for multiple units of this type with different orientation / irradiation on the collector field.
- Changed connection to IAM-data File (Omode 4) from Assign statement and LUI (did somehow not work anymore) to Label 1 and automatic Unit Number association.

Changes from V 3.08 to V 3.10

- A new multinode option has been introduced where the heat losses or gains towards or from ambient air are calculated based on the temperature difference of each single node to the ambient rather than taking the average of the inlet of the first node and the outlet of the last node for heat loss / gain calculation. This mode can be used to calculate a number of collectors in series and/or to get more consistent results for collector operation with low massflows and little or no irradiation.
- Maximum number of nodes has been increased to 100, and a stability check has been introduced to detect mass flows that are too low to produce a stable result.
- Condensation gains are now calculated based on Perers (2010) and based on Bertram et al. (2010). The possibility of sublimation (frosting) has been added to these calculations (attention, there is no validation of this feature and no subsequent melting or increased heat transfer resistance is calculated).

- Changed UAabsfl to Uabsfl (per m2) and used it also for calculation of surface temperature for Bertram condensation losses

Changes introduced with V 3.07 and V 3.08

The number of Parameters changed to 21 for optical modes Omode ≤ 5 and 109 for Omodes > 5 , where detailed data for incidence angle modifiers are included in the parameters. The main differences to earlier versions of this TRNSYS type are:

5. Possibility to split the collector into several segments for the calculation of the thermal mass temperature to avoid unexpected temperature jumps that had disturbed controllers and convergence in previous versions. These jumps were only significant when a collector with a relatively high thermal capacitance was simulated or when relatively small time steps were chosen for the simulation.
6. Possibility to calculate the transversal and longitudinal incidence angles from data readily available from the radiation processor of TRNSYS.
7. Several bugfixes were made addressing erroneous calculations and wrongly read IAM data files in previous versions when several instances of this Type were used in the same deck.
8. The quadratic heat loss term has been adapted in order not to calculate losses when the collector temperature is below ambient temperature. This does NOT mean that the collector model should be used for below ambient temperature operation.